

Classically optimized Hamiltonian simulation

Conor Mc Keever* and Michael Lubasch

Cambridge Quantum Computing Limited, SW1P 1BX London, United Kingdom

(Dated: May 24, 2022)

Hamiltonian simulation is a promising application for quantum computers to achieve a quantum advantage. We present classical algorithms based on tensor network methods to optimize quantum circuits for this task. We show that the classically optimized circuits can be orders of magnitude more accurate than Trotter product formulas.

I. INTRODUCTION

Quantum computers are expected to produce novel insights into quantum chemistry and materials [1–4] as they are believed to have an advantage over classical computers in performing Hamiltonian simulation, since powerful quantum algorithms for this task were discovered [5–9]. To make this type of simulation more efficient, there has been significant progress on the theoretical quantum algorithmic side [10–15] as well as on the more applied side of variational quantum algorithms [16–24]. However, the theoretical approaches can lead to deep quantum circuits and the variational approaches can require a large number of circuit runs in the optimization. Therefore Hamiltonian simulation is still challenging for current quantum devices [25–27].

In this article, our goal is to reduce the quantum hardware requirements for Hamiltonian simulation by performing quantum circuit optimization on a classical computer. To that end, we propose and analyze specific classical algorithms to approximate the time evolution operator by shallow quantum circuits. A previous proposal for this task focused on translationally invariant quantum systems and circuits [28]; we design our approach to be applicable to more general Hamiltonians and quantum circuits. We make use of tensor network techniques [29–31] to ensure the efficient scalability of our methods with qubit count. More specifically, we write the quantum circuits needed for the optimization in terms of products of matrix product operators (MPOs) [32, 33] and evaluate them by contracting the corresponding tensor networks. For the gate optimization, we compare the coordinate-wise approach in [22] to the Newton method. These techniques enable us to efficiently work with various shallow ansatz circuits, e.g. of brickwall and sequential structure, as well as with a large class of Hamiltonians, e.g. with open and periodic boundary conditions and with local and nonlocal interactions. Additionally, the algorithms are hardware-agnostic and can handle any set of native quantum gates. To illustrate the approach, we choose a brickwall circuit for the ansatz and an open quantum Ising chain with both transverse and longitudinal fields for the Hamiltonian. The performance of some of our algorithms is shown in Fig. 1.

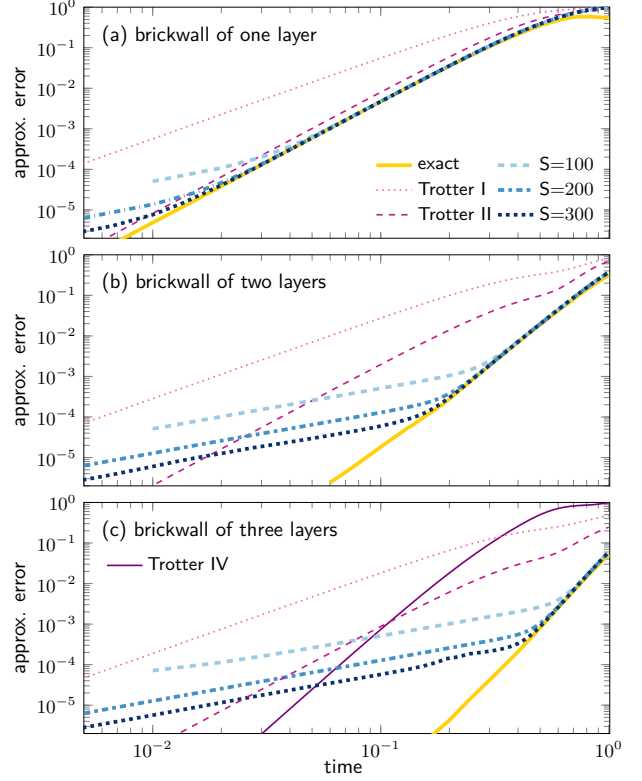


FIG. 1. Classically optimized Hamiltonian simulation (thick lines) vs. Trotter product formulas (thin lines) for a brickwall circuit of depth (a) one, (b) two, and (c) three. The approximation error, defined in Sec. II, of the approximate evolution operator U_{approx} with respect to the exact one $\exp(-itH)$ is shown as a function of time t . We consider $H = 2 \sum_{k=1}^7 Z_k Z_{k+1} + \sum_{k=1}^8 X_k + \sum_{k=1}^8 Z_k$. For the Trotter results U_{approx} is a Trotter product formula of 1st (dotted), 2nd (dashed) and 4th (solid) order. For the classically optimized results $U_{\text{approx}} = U(\theta)$ is the circuit with parameters θ after two optimization procedures: The first procedure minimizes the approximation error to the exact operator $\exp(-itH)$ (solid); the second procedure cuts the total time t into $S = 100$ (dashed), 200 (dash-dotted) and 300 (dotted) slices of equal time $\tau = t/S$ and then optimizes using a 1st order Taylor approximation of $\exp(-i\tau H)$ and S iterations thereof. We observe that by increasing S the results of the Taylor approach converge to the ones obtained via $\exp(-itH)$. Additionally we see that the classically optimized two- and three-layer circuits are two orders of magnitude more accurate than the Trotter formulas. Further details are in Sec. III.

* conor.mckeever@cambridgequantum.com

The article is structured as follows. Section II presents the algorithms and we analyse the results of our numerical experiments in Sec. III. A concluding discussion is given in Sec. IV.

II. METHODS

To approximate the time evolution operator $\exp(-itH)$ by a quantum circuit, we split the total evolution time t into S slices of equal size $\tau = t/S$ and then compute the circuit $U(\boldsymbol{\theta})$ for slice s by minimizing the cost function $\|U(\boldsymbol{\theta}) - \exp(-i\tau H)U_{s-1}\|_F^2$ over the variational parameters $\boldsymbol{\theta} = (\theta_1, \theta_2, \dots, \theta_K)$. Here $\|\cdot\|_F$ is the Frobenius norm, U_{s-1} the final circuit after optimization of the previous slice and $U_0 = \mathbf{1}$. The minimization of this cost function is equivalent to the maximization of the objective function

$$F(\boldsymbol{\theta}) = \text{Re}\{\text{tr}[U^\dagger(\boldsymbol{\theta}) \exp(-i\tau H)U_{s-1}]\} \quad (1)$$

where $\text{Re}\{\cdot\}$ denotes the real part, $\text{tr}[\cdot]$ the trace and $U^\dagger(\boldsymbol{\theta})$ is the adjoint of $U(\boldsymbol{\theta})$. We define the approximation error $\sqrt{1 - F(\boldsymbol{\theta})/2^n} \in [0, 1]$ for n qubits. Next we approximate $\exp(-i\tau H)$ by a truncated Taylor series and in our simulations use the MPO representation thereof [34]. This allows us to express the objective function as a product of MPOs as shown in Fig. 2.

We propose to use a Newton method to maximize the objective function in Eq. (1). This method requires the gradient vector \mathcal{G} with elements $\mathcal{G}_k = \partial F/\partial\theta_k$ and Hessian matrix \mathcal{H} with elements $\mathcal{H}_{j,k} = \partial^2 F/\partial\theta_j\partial\theta_k$ and iterates

$$\boldsymbol{\theta}^{(i+1)} = \boldsymbol{\theta}^{(i)} - \left(\mathcal{H}^{(i)}\right)^{-1} \mathcal{G}^{(i)}. \quad (2)$$

For the computation of the inverse of the Hessian matrix, we use that this matrix is Hermitian and that we are only interested in its negative eigenvalues, since our goal is the maximization of the objective function. Therefore we compute the pseudoinverse via the eigendecomposition of the Hessian matrix and by setting all eigenvalues larger than some cutoff $-\epsilon$ to zero.

As an alternative to the Newton method, we also consider a coordinatewise optimization method which for the type of objective function Eq. (1) was derived in [22]. The coordinatewise procedure updates variational parameters one after another and computes for each parameter:

$$\theta_k^{\text{new}} = \theta_k^{\text{old}} - 2\text{atan2}(F(\theta_k^{\text{old}}), F(\theta_k^{\text{old}} + \pi)) + 4\pi(p + \frac{1}{4}) \quad \forall p \in \mathbb{Z} \quad (3)$$

$$F(\theta_k^{\text{new}}) = \sqrt{(F(\theta_k^{\text{old}}))^2 + (F(\theta_k^{\text{old}} + \pi))^2}. \quad (4)$$

Here $\text{atan2}(y, x)$ returns the argument of the complex number $x + iy$. We use the simplified notation $F(\theta_k) = F(\theta_1, \dots, \theta_{k-1}, \theta_k, \theta_{k+1}, \dots, \theta_K) = F(\boldsymbol{\theta})$ for the objective function as a function of one specific parameter

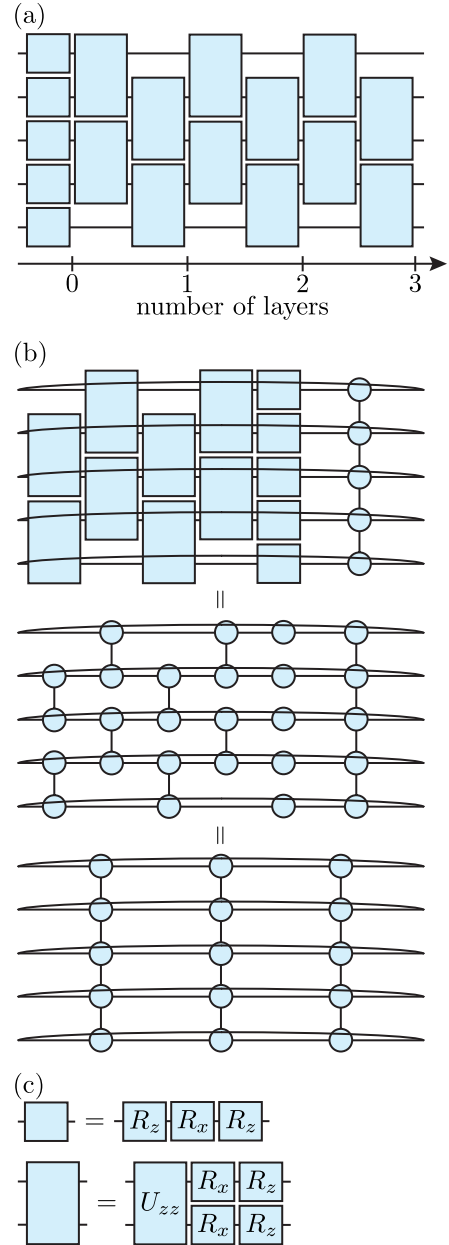


FIG. 2. (a) Brickwall ansatz for $n = 5$ qubits. (b) We rewrite the objective function Eq. (1) as a product of MPOs by, firstly, factorizing each two-qubit gate into a product of two tensors and, secondly, multiplying adjacent tensors into MPOs. (c) Parameterization in terms of the gates $R_x(\theta) = \exp(-i\theta X/2)$, $R_z(\theta) = \exp(-i\theta Z/2)$ and $U_{zz}(\theta) = \exp(-i\theta Z \otimes Z/2)$ where θ denotes the variational parameter.

θ_k under the assumption that all other parameters θ_j for $j \neq k$ are fixed. Note that $F(\theta_k^{\text{new}}) = F(\theta_{k+1}^{\text{old}})$. Therefore, after the first parameter update (for $k = 1$) we only need one evaluation of the objective function at $\theta_k^{\text{old}} + \pi$ (for $k > 1$) for each parameter update, because we know $F(\theta_k^{\text{old}}) = F(\theta_{k-1}^{\text{new}})$ from the previous parameter update.

III. RESULTS

We use the following setup in our numerical experiments. For the Hamiltonian we consider the transverse-field quantum Ising chain with an additional magnetic field and open boundary conditions:

$$H = J \sum_{k=1}^{n-1} Z_k Z_{k+1} + g \sum_{k=1}^n X_k + h \sum_{k=1}^n Z_k \quad (5)$$

where J , g and h are parameters of the Hamiltonian and X (Z) is the Pauli X (Z) matrix. For the quantum circuit ansatz we use the brickwall structure shown in Fig. 2 (a) composed of the gates shown in Fig. 2 (c). Newton's method is used with an eigenvalue cutoff of $\epsilon = 10^{-5}$ and iterated until the Euclidean norm of the vector of gradients falls below 10^{-5} . The tensor network calculations make use of the library [35].

We assess the performance of the coordinatewise approach and the Newton method by considering the approximation error achieved after successive iterations of the algorithms. For the coordinatewise method, one step of the algorithm corresponds to the update of a single variational parameter, whereas a single step of a global version of the Newton method updates all variational parameters at once. Between these two extremes we also perform the Newton method on a gate-by-gate and layer-by-layer basis, whereby only those variational parameters within a single gate or within a single layer, respectively, are updated simultaneously while all others remain fixed. To compare these methods, we plot in Fig. 3 the performance of successive iterations of each algorithm. We observe that the global Newton method converges to the lowest approximation error in the fewest number of just ten steps. In contrast, the coordinatewise method converges more slowly and produces a circuit with a larger approximation error. The Newton method on a gate-by-gate basis has a performance similar to that of the coordinatewise update while the Newton method on a layer-by-layer basis produces results which lie somewhere in between the global and local update methods.

Because the global Newton method performed best, in the following we use only this method in the classical optimization. We assess the performance of the classical algorithms by analyzing the results shown in Fig. 1. Let us first explain what is shown in Fig. 1. For a brickwall ansatz of one layer, a 1st order Trotter (Trotter I) and 2nd order Trotter (Trotter II) product formula is used as an approximation scheme [36]. The same is true for a brickwall ansatz of two layers, whereby two identical Trotter layers, each corresponding to an evolution by a time $t/2$, specify the circuit. Similarly, for a brickwall ansatz of three layers, three identical Trotter layers are composed to specify the circuit. Furthermore, a circuit of three layers allows us to also use a 4th order Trotter product formula (Trotter IV) [36]. The approximation errors of the Trotter based circuits are plotted in Fig. 1 and facilitate a fair comparison with the classically optimized

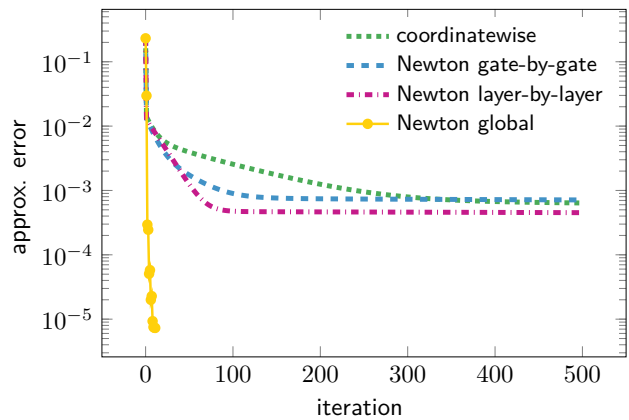


FIG. 3. Approximation error of the classically optimized circuit $U(\theta)$ with respect to the exact time evolution operator $\exp(-itH)$ achieved using various optimization algorithms. The variational parameters θ are initialized to zero and a single iteration corresponds to the update of all variational parameters in the circuit once. We consider the Hamiltonian in Eq. (5) with parameters $(J, g, h) = (2.0, 1.0, 1.0)$, time $t = 0.05$, $n = 8$ qubits and a brickwall circuit of two layers.

circuits inasmuch as the depth of two-qubit gates in the circuits considered within each subfigure – Fig. 1 (a), (b) and (c) – are the same.

In order to estimate how well the scalable optimization scheme can exhaust the potential of the brickwall circuits, we first optimize the variational circuit parameters for a cost function which is constructed using the exact unitary $\exp(-itH)$ and is calculated via matrix exponentiation. Supposing that the Newton based optimization scheme finds the global maximum of the objective function, these results (denoted exact in Fig. 1) give the minimum approximation error which can be achieved using the respective circuits. Compared to the Trotter based approximation schemes, the improvement using the exact scheme is small for a brickwall circuit of one layer (Fig. 1 a), however, deeper circuits (Fig. 1 b and c) lead to approximation errors which are orders of magnitude smaller than those obtained using Trotter product formulas.

The task of the Taylor based approach is to find circuit approximations as close as possible to the optimum achieved using the exact approach, in a manner which does not require exponentiation of the full Hamiltonian and is therefore scalable to larger system sizes. We find that the classical optimization scheme using a 1st order Taylor approximation is capable of finding variational parameters which approximate the target unitary with an approximation error equivalent to the exact scheme. This is evident in Fig. 1 where the exact and sliced Taylor ($S = 100$, $S = 200$, $S = 300$) results overlap, indicating that the approximation scheme has saturated the expressiveness of the circuit ansatz. Additionally, the time at which this saturation occurs falls earlier if more slices S are used.

In our calculations the Newton method typically re-

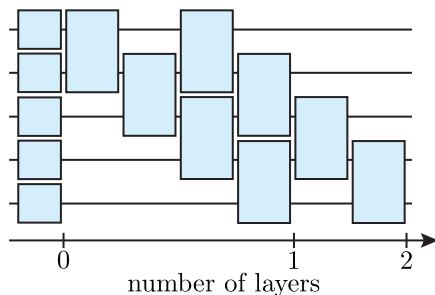


FIG. 4. Sequential quantum circuit for $n = 5$ qubits. One layer of the circuit can correlate qubits over the entire system size n , cf. with the brickwall ansatz in Fig. 2 (a) which requires order n layers to correlate qubits n sites apart.

quires around ten iterations per slice to converge and the most computationally expensive subroutines are the tensor contractions needed to compute the terms in the gradient vector and Hessian matrix. We note that the performance can be significantly improved by calculating these terms in parallel or by caching and reusing environment tensors.

The slopes of the data presented in Fig. 1 can be understood by considering the leading error arising from each approximating scheme. The leading errors of the Trotter product formulas are known to be of orders $O(t^2)$, $O(t^3)$ and $O(t^5)$ for the 1st, 2nd and 4th order Trotter product formulas, respectively, and this is apparent in the slope of the corresponding data presented in Fig. 1. For small times, the data for Trotter I, Trotter II and Trotter IV have slopes approximately equal to $m = 2$, $m = 3$ and $m = 5$, respectively.

The approximation errors arising from circuits which have been classically optimized via Taylor ($S = 100$, $S = 200$, $S = 300$) are based on a 1st order Taylor approximation. These curves are split into two regimes. The first regime occurs before the data overlap with those of the exact method and have a slope approximately equal to $m = 1$, indicating a leading error of order $O(t)$, as expected for the error accumulated by a 1st order Taylor approximation. The second regime occurs at larger times where the Taylor data overlap with the exact data. Here the corresponding slopes reflect the expressiveness of the circuits used. By fitting the data within this second regime and rounding to one decimal place, we find lead-

ing errors of orders $O(t^{3.0})$, $O(t^{4.5})$ and $O(t^{6.2})$ for brick-wall circuits of one, two and three layers, respectively. Therefore the classically optimized circuits of two and three layers are significantly more accurate than Trotter product formulas. We have also performed the same calculations for a system of $n = 5$ qubits (not shown) and the results were quantitatively similar.

IV. DISCUSSION

In this article we present classical algorithms that reduce the quantum hardware requirements for simulating the time evolution of quantum systems and we illustrate their performance for a local Hamiltonian with open boundary conditions using a variational brickwall quantum circuit. These algorithms can readily tackle a wider range of problems and optimize other types of quantum circuits. For example, periodic systems, Hamiltonians with nonlocal interactions or the sequential quantum circuit shown in Fig. 4 can be considered. Even shallow two-dimensional quantum circuits, as required by some of the IBM quantum devices, can be handled by making use of tensor network techniques for two-dimensional systems, e.g. [37–41].

To efficiently work with time evolution over long times, we cut the total time evolution into several slices and then represent the shorter time evolution per slice using a 1st order Taylor approximation. It is interesting to study more accurate approximations, e.g. a higher-order truncated Taylor series or perhaps a Jacobi-Anger expansion [42], that decrease the number of slices needed for a certain accuracy. Any approximation of the time evolution operator as a finite polynomial $\exp(-itH) \approx \sum_{r=0}^R \alpha_r H^r$ turns the objective function into a finite sum $F(\theta) = \text{Re}\{\text{tr}[U^\dagger(\theta) \exp(-itH)]\} \approx \sum_{r=0}^R \alpha_r \text{Re}\{\text{tr}[U^\dagger(\theta) H^r]\}$. The question is whether the additional cost of evaluating higher powers of H can still lead to a reduction of the overall cost due to the smaller total number of slices.

V. ACKNOWLEDGMENTS

We are thankful for valuable discussions with David Amaro, Marcello Benedetti, Yuta Kikuchi and Chris N. Self.

-
- [1] I. Kassal, J. D. Whitfield, A. Perdomo-Ortiz, M.-H. Yung, and A. Aspuru-Guzik, Simulating chemistry using quantum computers, *Annu. Rev. Phys. Chem.* **62**, 185 (2011).
- [2] Y. Cao, J. Romero, J. P. Olson, M. Degroote, P. D. Johnson, M. Kieferová, I. D. Kivlichan, T. Menke, B. Peropadre, N. P. D. Sawaya, S. Sim, L. Veis, and A. Aspuru-Guzik, Quantum chemistry in the age of quantum com-

- puting, *Chem. Rev.* **119**, 10856 (2019).
- [3] S. McArdle, S. Endo, A. Aspuru-Guzik, S. C. Benjamin, and X. Yuan, Quantum computational chemistry, *Rev. Mod. Phys.* **92**, 015003 (2020).
- [4] B. Bauer, S. Bravyi, M. Motta, and G. K.-L. Chan, Quantum algorithms for quantum chemistry and quantum materials science, *Chem. Rev.* **120**, 12685–12717 (2020).

- [5] S. Wiesner, Simulations of many-body quantum systems by a quantum computer (1996), [arXiv:quant-ph/9603028](#).
- [6] S. Lloyd, Universal quantum simulators, *Science* **273**, 1073 (1996).
- [7] D. S. Abrams and S. Lloyd, Simulation of Many-Body Fermi Systems on a Universal Quantum Computer, *Phys. Rev. Lett.* **79**, 2586 (1997).
- [8] C. Zalka, Simulating quantum systems on a quantum computer, *Proc. Math. Phys. Eng. Sci.* **454**, 313 (1998).
- [9] I. Kassal, S. P. Jordan, P. J. Love, M. Mohseni, and A. Aspuru-Guzik, Polynomial-time quantum algorithm for the simulation of chemical dynamics, *Proc. Natl. Acad. Sci. U.S.A* **105**, 18681 (2008).
- [10] D. W. Berry and A. M. Childs, Black-box hamiltonian simulation and unitary implementation, *Quantum Inf. Comput.* **12**, 29 (2012).
- [11] A. M. Childs and N. Wiebe, Hamiltonian simulation using linear combinations of unitary operations, *Quantum Inf. Comput.* **12**, 901 (2012).
- [12] D. W. Berry, A. M. Childs, R. Cleve, R. Kothari, and R. D. Somma, Simulating Hamiltonian Dynamics with a Truncated Taylor Series, *Phys. Rev. Lett.* **114**, 090502 (2015).
- [13] D. W. Berry, A. M. Childs, and R. Kothari, Hamiltonian Simulation with Nearly Optimal Dependence on all Parameters, in *2015 IEEE 56th Annual Symposium on Foundations of Computer Science* (2015) pp. 792–809.
- [14] G. H. Low and I. L. Chuang, Optimal Hamiltonian Simulation by Quantum Signal Processing, *Phys. Rev. Lett.* **118**, 010501 (2017).
- [15] G. H. Low and I. L. Chuang, Hamiltonian Simulation by Qubitization, *Quantum* **3**, 163 (2019).
- [16] Y. Li and S. C. Benjamin, Efficient variational quantum simulator incorporating active error minimization, *Phys. Rev. X* **7**, 021050 (2017).
- [17] X. Yuan, S. Endo, Q. Zhao, Y. Li, and S. C. Benjamin, Theory of variational quantum simulation, *Quantum* **3**, 191 (2019).
- [18] C. Cirstoiu, Z. Holmes, J. Iosue, L. Cincio, P. J. Coles, and A. Sornborger, Variational fast forwarding for quantum simulation beyond the coherence time, *npj Quantum Inf.* **6**, 1 (2020).
- [19] S.-H. Lin, R. Dilip, A. G. Green, A. Smith, and F. Pollmann, Real- and imaginary-time evolution with compressed quantum circuits, *PRX Quantum* **2**, 010342 (2021).
- [20] F. Barratt, J. Dborin, M. Bal, V. Stojevic, F. Pollmann, and A. G. Green, Parallel quantum simulation of large systems on small NISQ computers, *npj Quantum Inf.* **7** (2021).
- [21] Y.-X. Yao, N. Gomes, F. Zhang, C.-Z. Wang, K.-M. Ho, T. Iadecola, and P. P. Orth, Adaptive Variational Quantum Dynamics Simulations, *PRX Quantum* **2**, 030307 (2021).
- [22] M. Benedetti, M. Fiorentini, and M. Lubasch, Hardware-efficient variational quantum algorithms for time evolution, *Phys. Rev. Research* **3**, 033083 (2021).
- [23] S. Barison, F. Vicentini, and G. Carleo, An efficient quantum algorithm for the time evolution of parameterized circuits, *Quantum* **5**, 512 (2021).
- [24] K. Wada, R. Raymond, Y.-y. Ohnishi, E. Kaminishi, M. Sugawara, N. Yamamoto, and H. C. Watanabe, Simulating Time Evolution with Fully Optimized Single-Qubit Gates on Parameterized Quantum Circuits (2021), [arXiv:2111.05538 \[quant-ph\]](#).
- [25] A. Smith, M. Kim, F. Pollmann, and J. Knolle, Simulating quantum many-body dynamics on a current digital quantum computer, *npj Quantum Inf.* **5**, 106 (2019).
- [26] B. Fauseweh and J.-X. Zhu, Digital quantum simulation of non-equilibrium quantum many-body systems, *Quantum Inf. Process.* **20**, 138 (2021).
- [27] E. Gustafson, P. Dreher, Z. Hang, and Y. Meurice, Indexed improvements for real-time trotter evolution of a $(1 + 1)$ field theory using NISQ quantum computers, *Quantum Sci. Technol.* **6**, 045020 (2021).
- [28] R. Mansuroglu, T. Eckstein, L. Nützel, S. A. Wilkinson, and M. J. Hartmann, Variational Hamiltonian simulation for translational invariant systems via classical preprocessing (2021), [arXiv:2106.03680 \[quant-ph\]](#).
- [29] F. Verstraete, V. Murg, and J. Cirac, Matrix product states, projected entangled pair states, and variational renormalization group methods for quantum spin systems, *Adv. Phys.* **57**, 143 (2008).
- [30] R. Orús, A practical introduction to tensor networks: Matrix product states and projected entangled pair states, *Ann. Phys. (N. Y.)* **349**, 117 (2014).
- [31] M. C. Bañuls, Tensor Network Algorithms: a Route Map (2022), [arXiv:2205.10345 \[quant-ph\]](#).
- [32] F. Verstraete, J. J. García-Ripoll, and J. I. Cirac, Matrix Product Density Operators: Simulation of Finite-Temperature and Dissipative Systems, *Phys. Rev. Lett.* **93**, 207204 (2004).
- [33] M. Zwolak and G. Vidal, Mixed-State Dynamics in One-Dimensional Quantum Lattice Systems: A Time-Dependent Superoperator Renormalization Algorithm, *Phys. Rev. Lett.* **93**, 207205 (2004).
- [34] M. P. Zaletel, R. S. K. Mong, C. Karrasch, J. E. Moore, and F. Pollmann, Time-evolving a matrix product state with long-ranged interactions, *Phys. Rev. B* **91**, 165112 (2015).
- [35] J. Haegeman, [TensorKit.jl](#).
- [36] N. Hatano and M. Suzuki, Finding exponential product formulas of higher orders, in *Quantum Annealing and Other Optimization Methods* (Springer, Berlin, Heidelberg, 2005) pp. 37–68.
- [37] F. Verstraete and J. I. Cirac, Renormalization algorithms for quantum many-body systems in two and higher dimensions (2004), [arXiv:cond-mat/0407066 \[cond-mat.str-el\]](#).
- [38] M. Lubasch, J. I. Cirac, and M.-C. Bañuls, Unifying projected entangled pair state contractions, *New J. Phys.* **16**, 033014 (2014).
- [39] M. Lubasch, J. I. Cirac, and M.-C. Bañuls, Algorithms for finite projected entangled pair states, *Phys. Rev. B* **90**, 064425 (2014).
- [40] P. Czarnik, J. Dziarmaga, and P. Corboz, Time evolution of an infinite projected entangled pair state: An efficient algorithm, *Phys. Rev. B* **99**, 035115 (2019).
- [41] C. Mc Keever and M. H. Szymbalska, Stable iPEPO Tensor-Network Algorithm for Dynamics of Two-Dimensional Open Quantum Lattice Models, *Phys. Rev. X* **11**, 021035 (2021).
- [42] M. Abramowitz and I. A. Stegun, Handbook of mathematical functions, Applied Mathematics Series **55**, 62 (1966).